Biosensors and Bioelectronics 51 (2014) 280–285

Contents lists available at ScienceDirect

Biosensors and Bioelectronics

journal homepage: www.elsevier.com/locate/bios

Microfluidic biosensor for the detection of DNA by fluorescence enhancement and the following streptavidin detection by fluorescence quenching

Jun Wang [a,b,c,*], Michihiko Aki [d], Daisuke Onoshima [a,b,e], Kenji Arinaga [d], Noritada Kaji [a,b,d], Manabu Tokeshi [a,b,f], Shozo Fujita [d], Naoki Yokoyama [d], Yoshinobu Baba [a,b,e,g]

[a] Department of Applied Chemistry, Graduate School of Engineering, Nagoya University, Nagoya, Japan
[b] MEXT Innovative Research Center for Preventive Medical Engineering, Nagoya University, Nagoya, Japan
[c] Department of Chemical and Biological Engineering, Chalmers University of Technology, Göteborg, Sweden
[d] Fujitsu Laboratories Ltd., Tokyo, Japan
[e] FIRST Research Center for Innovative Nanobiodevice, Nagoya University, Nagoya 464-8603, Japan
[f] Division of Biotechnology and Macromolecular Chemistry, Graduate School of Engineering, Hokkaido University, Sapporo, Japan
[g] Health Technology Research Center, National Institute of Advanced Industrial Science and Technology (AIST), Takamatsu, Japan

ARTICLE INFO

Article history:
Received 15 May 2013
Received in revised form
16 July 2013
Accepted 30 July 2013
Available online 6 August 2013

Keywords:
Microfluidic biosensor
Fluorescence switching
Complementary ssDNA
Streptavidin

ABSTRACT

We reported an optical DNA/protein microfluidic sensor which consists of single stranded (ss) DNA-Cy3 probes on gold surface and simple line-shape microfluidic channel. These ssDNA-Cy3 probes with random sequence in bulk solution or on gold surface exhibits fluorescence enhancement after binding with complementary ssDNA (cssDNA) targets. Particularly it did not require complicated design or hairpin-like stem-loop conformation, which made it easier to be made and applied in analytes detection by fluorescence switching techniques. Using ssDNA-cy3 probes attached on gold surface in a microfluidic channel, strong fluorescence enhancement was measured by ssDNA with cssDNA binding or ssDNA with cssDNA–biotin binding. The following introduction of streptavidin resulted in fluorescence quenching (fluorescence decrease) because of the binding of hybridized DNA–biotin with streptavidin. This sensor showed strong affinity and high sensitivity toward the streptavidin, the minimum detectable concentration for streptavidin was 1 pM, equating to an absolute detection limit of 60 amol in this microfluidic channel. Microfluidic channel height and flow rate is optimized to increase surface reaction efficiency and fluorescence switching efficiency. In contrast to previously reported optical molecular beacon approach, this sensor can be used not only for the detection of cssDNA target, but also for the detection of streptavidin. This microfluidic sensor offers the promise of analyzing kinds of molecular targets or immunoreactions.

1. Introduction

In recent years, the interest for DNA or protein-based diagnostic tests has been growing. The development of sensors allowing DNA or protein detection is motivated by applications in many fields: DNA diagnostics, gene analysis, fast detection of biological warfare agents, and forensic applications (Csako, 2006; Han et al., 2013; Tsongalis and Coleman, 2006; Epstein et al., 2002; Yeung et al., 2008). Numerous DNA detection systems based on the hybridization between a DNA target and its complementary probe, which is present either in solution or on a solid support, have been described (Heller, 2002; Bowtell, 1999; Winzeler et al., 1999; Cooper et al., 2001; Park et al., 2002; Livak, 1999; Lipshutz et al., 1999; Albert et al., 2009). Now the high importance is the need for techniques that do not require labeling of the target sample, because that increases the time, cost, and potential for error inherent in the analysis. In the context of solution-phase assays, the molecular beacon concept based fluorescence switching has proven itself to be both sensitive and reliable for their use as sensors for DNA sequencing (Broude, 2002; Dai et al., 1997; Heyduk and Heyduk, 2002; Tyagi and Kramer, 1996). Besides solution phase use, DNA hairpin probes have been immobilized onto solid substrates (Piestert et al., 2003; Liu and Tan, 1999; Fang et al., 1999). However, most of these employ an attached single molecule as quencher, while the material on which the hairpin is immobilized serves only a passive role, the substrates served only as an anchor: the function of the probe was unchanged from the solution assays.

Several groups have used gold substrate as a more efficient quenching agent instead of a quencher dye molecule for a surface-immobilized hairpin stem-loop single stranded DNA (ssDNA)

* Corresponding author at: Nagoya University, Furo-cho, Chikusa-ku, Nagoya 464-8603, Japan. Fax: +81 52 789 5499.
E-mail address: wjzyy988@gmail.com (J. Wang).

0956-5663/$ - see front matter © 2013 Elsevier B.V. All rights reserved.
http://dx.doi.org/10.1016/j.bios.2013.07.058

labeled with just one donor dye, which can be used for the detection of complementary DNA (cssDNA) target (Du et al., 2003; Fan et al., 2003). The oligonucleotide is designed in such a way that, in the absence of complementary DNA, the oligonucleotide will fold onto itself forming a hairpin like stem-loop structure. In this case, the fluorescent label at the end of ssDNA probes will be brought in close proximity to the gold surface, and its fluorescence will be quenched by the gold through a resonance energy transfer or "contact quenching" process. However, this method need to give a subtle design and detailed computation for the immobilized DNA which should form a hairpin-like stem-loop loop conformation which make the fluorescent dye in close proximity to the gold surface.

As reported, other alternatives for molecular beacons are developed, such as "Light-up probes", which is useful for the detection of cssDNA (Svanvik et al., 2000; Ghosh et al., 2006; Menacher et al., 2008; Yao and Tan, 2004). Recently, Abstreiter et al. have found that fluorescence enhancement effect occurs upon hybridization in bulk solution when using ssDNA probes modified with cyanine dye and without a quencher dye. This kind of probe had been applied for the construction of electrochemical sensor for cssDNA detection (Rant et al., 2007). In a previous study (Wang et al., 2011), we constructed an optical sensor for the detection of DNA binding proteins based on fluorescence quenching, however, the binding between DNA and DNA binding proteins in this experiment is non-specific reaction. Rant et al. (2009) discovered that the binding of antibody proteins by functionalized DNA layer on gold surface can cause fluorescence changes by the application of high frequency electrical potential. Therefore, the further study of specific binding reaction will be potential useful for immunoassay. For example, the interaction of biotin and streptavidin has been exploited for use in many protein and nucleic acid detection and purification methods.

In this study, we reported the detection of cssDNA target and the following streptavidin determination based on fluorescence enhancement and fluorescence quenching in our constructed microfluidic channel, wherein we attach ssDNA-Cy3 probes without hairpin loop structure on a gold substrate to achieve the detection of cssDNA or cssDNA–biotin by fluorescence enhancement. Subsequently, after fluorescence intensity reaches a stable state by the introduction cssDNA–biotin, the addition of streptavidin can be determined by the fluorescence quenching effect.

2. Experimental

2.1. Reagents and materials

The immobilized ssNA-Cy3 probe, cssDNA target and the cssDNA–biotin (at 5′ end connected with biotin) was obtained from Tsukuba Oligo Service Corporation (Tsukuba, Japan), the 48-mer ssDNA-Cy3 probe sequence is: 5′-HS-(CH_2)6-TAG TCG TAA GCT GAT ATG GCT GAT TAG TCG GAA GCA TCG AAC GCT GAT-Cy3-3′, the sequence of cssDNA or cssDNA–biotin are complementary to the sequence of ssDNA-Cy3. These DNA sequences are non-self-complementary and complicating secondary structures are not known. 6-Mercaptohexanol and streptavidin were purchased from Sigma-Aldrich chemical company (Saint Louis, USA) and used without further purification. All H_2O used in the preparation of buffers and for rinse solutions had a resistivity of 18.2 MΩ cm, produced by Milli-Q purification system (Billerica, USA). Gold substrate was provided by Fujitsu company (Tokyo, Japan): gold lines of 200 μm width were prepared on 3-in. single crystalline sapphire wafers by subsequently depositing thin layers of Ti (10 nm), Pt (40 nm), and Au (200 nm) using standard optical lithography and metallization techniques.

2.2. Fabrication of a microfluidic chip

Silicon wafers with positive surface reliefs were used as a mold master for the preparation of polydimethylsiloxane (PDMS) microfluidic channel, the positive reliefs with different height (5–450 μm) on the silicon wafer are prepared by varying the speed of spin coating or using the multi-layer coating techniques based on traditional photolithography method (Onoshima et al., 2012), Then the straight PDMS microfluidic channel with different height were prepared by the PDMS kit, PDMS base material and curing agent were mixed in 10:1 ratio, stirred vigorously for 15 min, and then degassed for 1 h under dynamic vacuum to remove all air bubbles. The clear solution was poured onto a vertical-shaped positive mold, heated at 75 °C for 1 h. After cooling, the PDMS microfluidic chip was peeled off from the mold. The PDMS microchip is equipped with two holes (2 mm diameter) directly above the microfluidic channel for sample transfer and connection of syringe pump.

2.3. Immobilization of DNA probe on Au surface

One layer of single-stranded oligonucleotides with non-self-complementary sequence was prepared on gold surface by adsorption from aqueous solution. The 5′ end of DNA probe was modified with a thiol linker to graft the strands chemically to the surface (S-Au bond). Single-stranded oligonucleotides that are end-grafted to a gold surface constitute the sensor′s basic element. Optimal surface densities are a mandatory prerequisite to the sensor, Before DNA adsorption, the Au surface were cleaned by Piranha solution (H_2SO_4: H_2O_2=7:3) and exposed to HNO_3 (60%) for 15 min each, followed by a final rinse with de-ionized water. The preparation of the DNA film proceeded in two steps. First, a relatively dense layer of thiol-modified oligonucleotides was formed on the gold surface by the attachment of HS-ssDNA-Cy3 from solution (immobilization solution: 1 μM HS-ssDNA-Cy3 containing 10 mM Tris and 50 mM NaCl, pH 7.4) for 1 h, after washed by distilled water, followed by the co-adsorption of short spacer molecules (1 mM mercaptohexanol containing 10 mM Tris and 50 mM NaCl, pH 7.4) for 1 h to improve the DNA layer structure and passivate the remaining gold surface. Following the immobilization the gold surface was further rinsed by distilled water, and dried by nitrogen gas for the later use.

2.4. Fluorescence detection by microscopy

Fluorescence images of immobilized ssDNA-cy3 probes on the gold surface in a microfluidic channel were obtained from a Nikon confocal microscope equipped with a silicon intensified target (SIT), the excitation was at 532 nm through a 0.45 NA, 20 × objective. Fluorescence images were collected through the same objective and passed through a dichroic beam splitter and a band-pass filter (575 nm) and imaged with SIT. While under laser illumination, the cssDNA was introduced by syringe pump at a desired flow rate, the fluorescence images was recorded with time. The fluorescence intensity increase or decrease data are obtained from the SIT images by the Adobe premiere and Cosmos software.

3. Results and discussion

3.1. Fluorescence enhancement by ssDNA-Cy3 and cssDNA binding in bulk solution

The ssDNA-Cy3 used in this experiment is designed in random sequence, it appear low fluorescence in the absence of cssDNA. After hybridization with cssDNA, the fluorescence intensity increase. Fig. 1 shows the fluorescence emission spectra of ssDNA-cy3 with cssDNA at different hybridization ratio. Fluorescence intensity increase when

the hybridization reaction starts, and fluorescence intensity changing with the increased hybridization ratio, which shows that this kind of ssDNA with random sequence labeled with Cy3 can be used as molecular beacon for the application for "label-free" detection of cssDNA in bulk solution. In the absence of their complement, these ssDNA-Cy3 probes exist in a closed, relative "dark" conformation. Hybridization occurs upon introduction of complementary oligonucleotides, which causes a fluorescent increase, "bright" state. However the principle for the change of fluorescence is not well understood, as we have said in the introduction, we think this fluorescence enhancements attributed to the conformation changes of Cy3 caused by hybridization, which maybe also can attributed to fluorescence resonance energy transfer or electron energy transfer (Ray et al., 2006). We tried this experiment in bulk solution and on gold surface with different nucleoid length (24-mer and 72-mer) of ssDNA-Cy3, fluorescence enhancement also exists after binding with cssDNA (data is shown in Figs. s1 and s2 of supplementary file), which agreed with previous paper (Rant et al., 2007, 2009). The salt concentration and pH in working buffer will affect the optimal fluorescence signal for this hybridization reaction. In order to have strong, sensitive and accurate fluorescence signals to observe the fluorescence switching of this ssDNA-Cy3 during nucleic hybridization process, the fluorescence signal was optimized to achieve maximum value. The optimized buffer conditions for this hybridization process are 10 mM Tris–HCl, 200 mM NaCl in pH 7.4 at room temperature. All working buffer used in this research were implemented in this optimized condition, if not explicitly mentioned.

3.2. *Principle of this microfluidic sensor for the detection of cssDNA and streptavidin*

An ssDNA-Cy3 modified with a thiol group at its 5′ end is attached onto a gold line on the 4-in. sapphire wafer, after washing with distilled water, PDMS microfluidic chip is put on the gold line

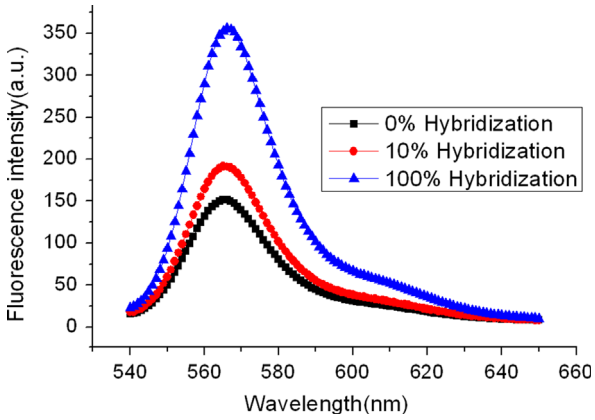

Fig. 1. Fluorescence spectra of ss-DNA-Cy3 at different hybridization ratio with cssDNA.

to construct a microfluidic biosensor (Fig. 2A), cssDNA target or streptavidin flow were introduced to react with ssDNA-Cy3 probes on gold surface in this microfluidic channel by syringe pump. SEM pictures of PDMS microfluidic channels and one optical graph of this microfluidic biosensor are shown in Fig. s3 of supplementary file. Fig. 2B shows the basic schematic of fluorescence enhancement and fluorescence quenching by the cssDNA or streptavidin protein. By the attachment of our ssDNA-Cy3 probes on gold surface, the Cy3 at the 3′ end of ssDNA may be brought in close proximity to the gold surface because of the bend or flexibility of ssDNA, and its fluorescence will be quenched by the gold through a resonance energy transfer or "contact quenching" process. Upon hybridization to cssDNA target or cssDNA–biotin target, the hybridized DNA or DNA–biotin will appear high fluorescence intensity which resulted from two reasons. First, the fluorescence enhancement is resulted from the rigid and rod-like qualities of double stranded DNA (dsDNA), which will stand up from the gold rendering Cy3 separated from the gold and eliminating the resonance energy transfer of Cy3 to gold. Second, it is the ssDNA-Cy3 probes itself. Due to these two reasons, this kind of ssDNA-Cy3 without hairpin loop structure may be more effective than previously reported optical sensor using ssDNA probes with complicated design that is specific for the proximity to gold.

After fluorescence intensity increases to a stable state by the fluorescence enhancement effect of cssDNA–biotin, the streptavidin flow is introduced to the sensor, the reaction of biotin–streptavidin can influence the conformation of dsDNA-Cy3 or the occurrence of the resonance energy transfer from Cy3 to the streptavidin protein, in turn cause fluorescence quenching effect. The overall fluorescence intensity recorded from all the excited dye molecules reflects the extent of the hybridization or biotin–streptavidin reaction.

The changes of fluorescence intensity can be obtained from the images of microscopy. Fig. 3 shows a typical curve of fluorescence intensity with the time by the introduction of cssDNA–biotin and subsequently introduction of streptavidin, it is divided by three parts: first, the blank fluorescence intensity (<0 min, left inset) is obtained using the buffer (10 mM Tris–HCl, pH 7.4, 200 mM NaCl) flow in the microfluidic channel; second, curve of fluorescence enhancement for the hybridization process is obtained (0–35 min) by the introduction of cssDNA–biotin flow, fluorescence intensity can reach a steady state or saturation state (middle inset) at the end; finally, the streptavidin flow is introduced to the microfluidic sensor and the curve of fluorescence quenching is obtained after 35 min, another fluorescence steady state by fluorescence quenching can be obtained (right inset). The three inset pictures are SIT images of DNA probes on the gold surface in the microfluidic channel under laser illumination: (a) blank image in buffer after ssDNA immobilization; (b) steady state image after hybridization reaction by cssDNA–biotin; (c) quenching steady state image by the streptavidin. The differences among the three processes is clear, the fluorescence enhancement effect and quenching effect can occur in these processes, which can be helpful for the detection of cssDNA target or protein. In this figure, F^I shows the

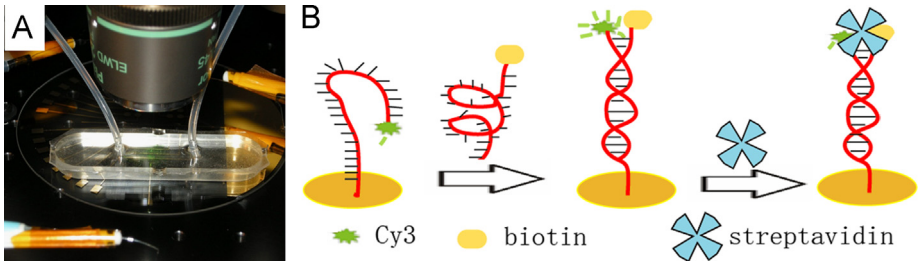

Fig. 2. (A) Optical micrograph of microfluidic biosensor; (B) schematic for the detection of target cssDNA and streptavidin on gold surface.

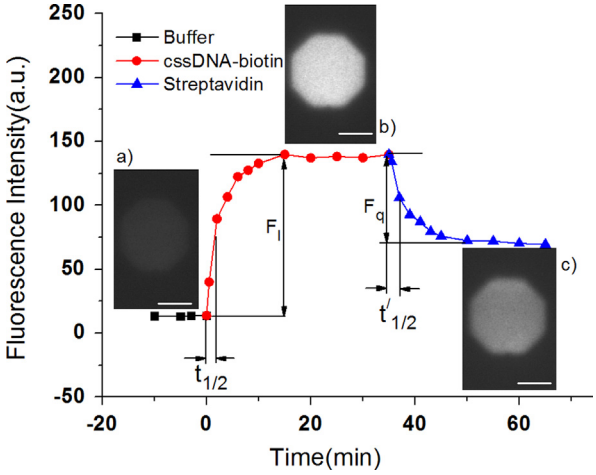

Fig. 3. Fluorescence intensity curve with time in this sensor after the introduction of cssDNA–biotin and streptavidin (SA), the intensity data is derived from the SIT images before cssDNA–biotin hybridization ((a) left inset, scale bar: 100 μm), after cssDNA–biotin derivation ((b) middle inset, scale bar: 100 μm) and after biotin–streptavidin reaction ((c) right inset, scale bar: 100 μm).

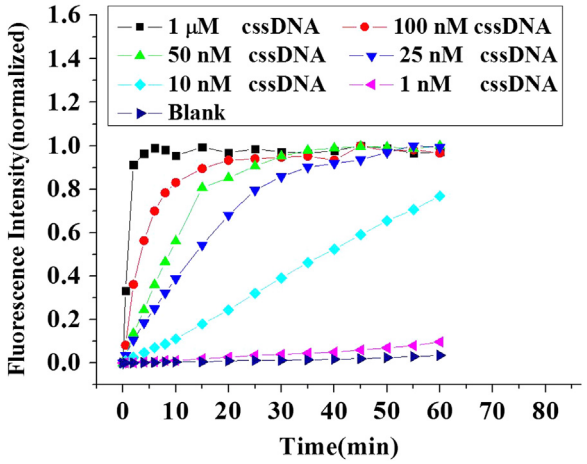

Fig. 4. Fluorescence intensity changes with time by introducing different concentrations of cssDNA in microfluidic channel.

value of maximum fluorescence enhancement from the blank baseline to the fluorescence steady state by the hybridization reaction. The time, $t_{1/2}$, shows the time required to reach 50% maximal fluorescence enhancement from the blank baseline; Fq shows the value of maximum fluorescence quenching influenced by the streptavidin, $t'_{1/2}$ shows the time required to reaching 50% maximum fluorescence quenching. As a result of the direct method used here, the real-time data contains the information about the hybridization reaction kinetics and streptavidin binding kinetics.

3.3. *Detection of cssDNA and streptavidin in this microfluidic sensor*

Microfluidic channel is ideally suited for the continuous monitoring of a flow of analytes, when the cssDNA flow is introduced into microfluidic channel, fluorescence intensity changes with flow time (Fig. 4). cssDNA concentration plays an important role in hybridization efficiency and fluorescence enhancement, which can be used for the quantitatively determination of cssDNA, the concentration of cssDNA is also key for the fluorescence quenching in the following step. Fig. 4 shows the relative fluorescence intensity increase differently at different concentration of cssDNA. When using 10 nM cssDNA, the fluorescence intensity cannot reach the steady fluorescence intensity and resulted in weak fluorescence, whereas at higher concentrations the dye fluorescence increased to the saturation in a nonlinear fashion. But the line shape in different concentration is similar as a simple solution-phase binding model described by others. A rapid initial hybridization rate was observed as a function of time after introduction the flow of higher concentration of cssDNA, we found a 50% maximal relative fluorescence intensity increase was obtained in approximately 15 min of introduction of cssDNA between 25 nM and 1 μM, and steady state was reached in less than 2 h for the concentration of cssDNA between 10 nM and 1 μM.

Microfluidic sensors for the protein assay with sufficient sensitivity are useful analytical tools for detection of biological important substances. Because of the minimized handling of hazardous materials, short reaction times, portability and versatility in design, and capability for parallel operation, microfluidics is used extensively to deliver sample to reaction sites where binding of target and analyte molecules take place (Manz et al., 1990; Reyes et al., 2002). Here, as a model of immunoassay determination, we applied this sensor to detect the streptavidin based on the hybridization of cssDNA–biotin with the probes on gold. For the determination of streptavidin, we first introduce 100 nM cssDNA–biotin to start the hybridization reaction because the fluorescence intensity can quickly reach to the steady state in less than 20 min.

Table 1
Fluorescence quenching affected by different microfluidic parameters (channel height, channel flow rate).

Channel height/μm	Linear velocity/(cm/s)		$t'_{1/2}$/min	
5	5	↑	2	
	1.67		2	
	0.38		2	
10	5	↑	3	
	1.67		3	
	0.38		3	
25	5	↑	2	↓
	1.67		4	
	0.38		5	
65	5	↑	3	↓
	1.67		6	
	0.38		8	

The flow-rate and channel dimensions are parameters usually overlooked in system optimization. In considering these, it is possible to enhance detection performance of our sensor without increased cost in detector requirements. Table 1 shows the results of fluorescence quenching process influenced by channel height and flow rate upon introduction of streptavidin. By introducing a sample flow to a deeper microfluidic channel, the quenching efficiency can be enhanced, allowing more target molecules interact with the binding site, significantly reducing hybridization times, however, for the shallow microchannel, the quenching time ($t'_{1/2}$) can have a steady state for different linear velocity, which probably because of the diffusion limitation in the shallow channel. Reducing the channel height improves the system hybridization efficiency and quenching efficiency, limiting the travel of molecules due to diffusion. For the sake of decreasing the sample consumption, we choose the microfluidic channel (5 μm depth and 200 μm width) and 1 μl/min flow rate for the cssDNA and protein sample flow. After optimization, the sensor in microfluidic format not only provides the method to adjust the surface reaction efficiency but also provides a potentially more efficient approach to control and automate sample introduction and steps such as washing and reagent addition.

The fluorescence intensity changes with the introduction of streptavidin are showed in Fig. 5A. Fluorescence quenching occurs by the introduction of streptavidin from 0 min to 60 min

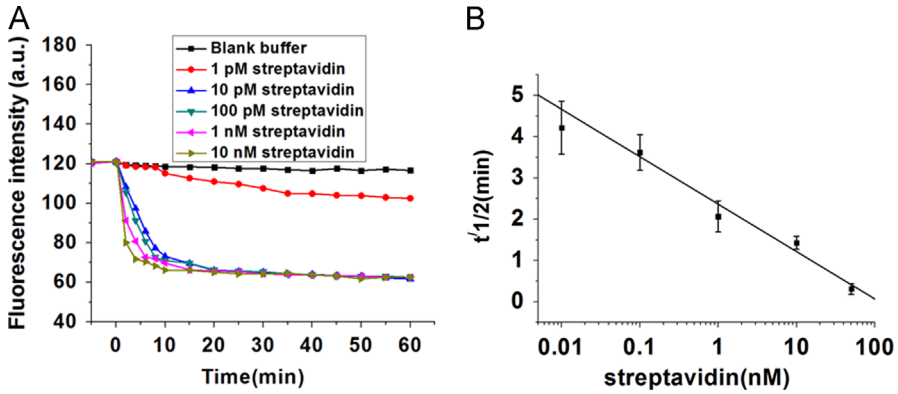

Fig. 5. (A) Fluorescence quenching by different concentrations of streptavidin in sensor; (B) dose response curve of streptavidin with half quenching time at the concentration from 10 pM to 50 nM.

(fluorescence intensity before 0 min as background). No significant fluorescence quenching is observed for the introduction of streptavidin-free hybridization buffer flow, while the introduction of 1 pM and 1 nM streptavidin can cause the fluorescence quenching phenomena, which suggests the feasibility of this sensor for protein detection. Under these conditions, we observe easily measurable decreases in fluorescence intensity at streptavidin concentrations as low as 1 pM. We currently employ a sample volume of 60 μl, equating to an absolute detection limit of 60 amol, which is comparable to or significantly better than normal sensor or electrochemical sensor (Fang et al., 1999).

The convection time or diffusion time of protein on the gold surface also influences the Fq and $t^{l}_{1/2}$ value, we found the similar effect by the higher concentration of streptavidin as the introduction of higher concentration of cssDNA (data not shown). The maximum fluorescence quenching value, Fq, can be reached to the same value at the concentration higher than 10 pM at less than 10 min, which attributed our continuous introduction of protein which cause the same diffusion effect in the microfluidic channel. Because the flow rate of streptavidin is 1 μl/min, the consumption of streptavidin for the DNA–biotin on the surface is about 10^{-16} mol, corresponds to a detection limit of 6×10^{7} streptavidin target recognitions in this sensor. For comparison, this value is better than other label-free methods, surface plasma resonance DNA sensors (Yu et al., 2004), and almost three orders of magnitude and approaches the limit of assays using dye-labeled targets. When the lower concentration of streptavidin (for example 1 pM) is introduced, because the convection time of protein is lower than the diffusion time, streptavidin in the channel are more difficult to "reach" the reactive surface exiting the sensing region and low fluorescence quenching.

Here, the quenching time $t^{l}_{1/2}$ exhibits concentration dependent feature, which can be used for the quantitative determination of streptavidin. Fig. 5B shows the linear correlation between the concentration of streptavidin and the half quenching time and the concentration of streptavidin in the concentration from 10 pM to 50 nM, spanning a response region of 4 orders of magnitude. Results also showed a linear decrease in half quenching time with increasing streptavidin concentration up to 50 nM ($R^2=0.99$).

This sensor can produce an easily measurable output signal for streptavidin upon the biotin–streptavidin reaction, after the hybridization of cssDNA–biotin in the microfluidic sensor. But these operational steps might be simplified by the directly immobilization dsDNA–biotin. This strategy to the detection of streptavidin by this label-free sensor through DNA hybridization principle provides the promise for the detection of other biomolecules or reactions by the subsequent fluorescence quenching. The other non-specific proteins (bovine serum protein and lysozyme) were also tried by this microfluidic biosensor, high concentration of BSA or lysozyme can only cause less than 1% of fluorescence quenching effect on double stranded DNA-Cy3 probes (as shown in Fig. s4 of supplementary file), which demonstrates the potential for the further investigation of other proteins by this microfluidic biosensor based on the antibody–antigen reaction.

4. Conclusion

The ssDNA-Cy3 without terminally attached quencher molecule and complicated hairpin-like stem-loop structure has been developed as optical molecular beacon, which shows fluorescence enhancement effect on hybridization with cssDNA in a bulk solution. Combining this attached ssDNA-Cy3 probes on the gold and microfluidic techniques, we developed a microfluidic sensor and proved its feasibility for the detection of cssDNA target based on fluorescence enhancement by the hybridization reaction. Particularly, after the hybridization reaction of cssDNA–biotin, the fluorescence signal can be quenched by the biotin–streptavidin reaction for the determination of streptavidin. Microfluidic channel height and flow rate can influence the reaction efficiency and is optimized for the protein detection, which provides a potentially more efficient approach to control and automate sample introduction and surface reaction. This sensor can perform continuous detection of analytes in a flowing matrix and achieve high sensitivity with low sample consumption. The strategy of this sensor may be generalized to other reaction and serve as technical platinum for DNA or protein detection. This approach is also potential for the application of multiplex detection or continuous monitoring of label-free sample flow.

Appendix A. Supplementry material

Supplementary data associated with this article can be found in the online version at http://dx.doi.org/10.1016/j.bios.2013.07.058.

References

Albert, T.H., Patrick, J.P., Abraham, P.L., 2009. Microfluidics and Nanofluidics 6, 391–401.
Bowtell, D.D.L., 1999. Nature Genetics 21, 25–32.
Broude, N.E., 2002. Trends in Biotechnology 20, 249–256.
Csako, G., 2006. Clinica Chimica Acta 363, 6–31.
Cooper, M.A., Dultsev, F.N., Minson, T., Ostanin, V.P., Abell, C., Klenerman, D., 2001. Nature Biotechnology 19, 833–837.

Dai, X., Greizerstein, M.B., Nadas-Chinni, K., Rothman-Denes, L.B., 1997. Proceedings of the National Academy of Sciences of the United States of America 94, 2174–2179.
Du, H., Disney, M.D., Miller, B.L., Krauss, T.D., 2003. Journal of the American Chemical Society 125, 4012–4013.
Epstein, J.R., Biran, I., Walt, D.R., 2002. Analytica Chimica Acta 469, 3–36.
Fang, X., Liu, X., Schuster, S., Tan, W., 1999. Journal of the American Chemical Society 121, 2921–2922.
Fan, C., Plaxco, K.W., Heeger, A.J., 2003. Proceedings of the National Academy of Sciences of the United States of America 100, 9134–9137.
Ghosh, I., Stains, C.I., Ooi, A.T., David, J.S., 2006. Molecular Biosystems 2, 551–560.
Han, K.N., Li, C.A., Seong, G.H., 2013. Annual Review of Analytical Chemistry 6, 119–141.
Heller, M.J., 2002. Annual Review of Biomedical Engineering 4, 129–153.
Heyduk, T., Heyduk, E., 2002. Nature Biotechnology 20, 171–176.
Livak, K.J., 1999. Genetic Analysis-Biomolecular Engineering 14 (5/6), 143–149.
Lipshutz, R.J., Fodor, S.P., Gingeras, T.R., Lockhart, D.J., 1999. Nature Biotechnology 21, 20–24.
Liu, X., Tan, W., 1999. Analytical Chemistry 71, 5054–5059.
Menacher, F., Rubner, M., Berndl, S., Wagenknecht, H., 2008. Journal of Organic Chemistry 73, 4263–4426.
Manz, A., Graber, N., Wildmer, H.M., 1990. Sensors and Actuators B: Chemical 1, 244–248.
Onoshima, D., Wang, J., Aki, M., Arinaga, K., Kaji, N., Tokeshi, M., Fujita, S., Yokoyama, N., Baba, Y., 2012. Analytical Methods 4, 4368–4372.
Park, S.J, Taton, T.A., Mirkin, C.A., 2002. Science 295, 1503–1506.
Piestert, O., Barsch, H., Buschmann, V., Heinlein, T., Knemeyer, J.P., Weston, K.D., Sauer, M., 2003. Nano Letters 3, 979–982.
Rant, U., Arinaga, K., Scherer, S., Pringsheim, E., Fujita, S., Yokoyama, N., Tornow, M., Abstreiter, G., 2007. Proceedings of the National Academy of Sciences of the United States of America 104 (44), 17364–17369.
Rant, U., Pringsheim, E., Kaiser, W., Arinaga, K., Knezevic, J., Tornow, M., Fujita, S., Yokoyama, N., Abstreiter, G., 2009. Nano Letters 4, 1290–1295.
Ray, P.C., Fortner, A., Darbha, G.K., 2006. Journal of Physical Chemistry B 110, 20745–20748.
Reyes, D.R., Iossifidis, D., Auroux, P.A., Manz, A., 2002. Analytical Chemistry 74, 2623–2636.
Svanvik, N., Westman, G., Wang, D.Y., Kubista, M., 2000. Analytical Biochemistry 281, 26–35.
Tsongalis, G.J., Coleman, W.B., 2006. Clinica Chimica Acta 363, 127–137.
Tyagi, S., Kramer, F.R., 1996. Nature Biotechnology 14, 303–308.
Winzeler, E.A., Schena, M., Davis, R.W., 1999. Methods in Enzymology 306, 3–18.
Wang, J., Onoshima, D., Aki, M., Okamoto, Y., Kaji, N., Tokeshi, M., Baba, Y., 2011. Analytical Chemistry 83, 3528–3532.
Yeung, S.H.I., Medintz, I.L., Greenspoon, S.A., Mathies, R.A., 2008. Clinical Chemistry 4 (6), 1080–1084.
Yao, G., Tan, W.H., 2004. Analytical Biochemistry 331 (2), 216–223.
Yu, F., Yao, D., Knoll, W., 2004. Nucleic Acids Research 32, e75.